Performance of TerraSAR-X for urban subsidence monitoring: Murcia case study

Daniel Monells, Remote Sensing Lab.-UPC, Spain
Giuseppe Centolanza, Remote Sensing Lab.-UPC, Spain
Jordi J. Mallorqui, Remote Sensing Lab.-UPC, Spain
Sergi Duque, Remote Sensing Lab.-UPC, Spain
Roberto Tomás, Universidad de Alicante (UA), Spain
Juan M. Lopez-Sanchez, Universidad de Alicante (UA), Spain
Fernando Vicente, Universidad de Alicante (UA), Spain
Gerardo Herrera, Instituto Geológico y Minero (IGME), Spain
Joaquín Mulas, Instituto Geológico y Minero (IGME), Spain

Abstract

This paper presents an analysis of the performance of TerraSAR-X for subsidence monitoring in urban areas. The city of Murcia has been selected as a test-site due to its high deformation rate and the set of extensometers deployed along the city that provide validation data. The obtained results have been compared with those obtained from ERS/ENVISAT data belonging to the same period and validated with the in-situ measurements.

1 Introduction

Orbital DInSAR is a technique widely used to survey the surface of the Earth and monitor hazards due to natural and human agents, such as earthquakes or mining [1][2][3]. Nowadays, there are a large number of satellites in orbit carrying SAR instruments able to perform this monitoring. In this work we will make a comparison of the results of urban subsidence monitoring obtained using data from veteran satellites ERS-2 and ENVISAT and the new satellite TerraSAR-X. The objective of the paper is to compare the performance of each system under different aspects, such as the management and detection of different kinds of targets (distributed or deterministic), the preservation of the coherence/phase stability and its temporal evolution, and a comparison of the deformation results using each set of data.

2 The Coherent Pixels Technique (CPT)

The Coherent Pixels Technique has been widely used for monitoring urban subsidence [3]. The algorithm can use both coherence and amplitude stability criteria to perform pixels selection. The former is more suited for detecting stable distributed targets and the latter for detecting the so-called Permanent Scatterers (PS). The retrieval of the deformation time-series is done in two steps. Firstly, a linear model adjustment to data provides the linear velocity of deformation, the DEM error and the azimuth position of the PS (only for amplitude-based processing when large Dopplers are present). Secondly, the non-linear processing retrieves the non-linear deformation and the atmospheric phase screen for each image.

3 The city of Murcia test-site

Subsidence has occurred in the metropolitan area of Murcia City (SE Spain) as a result of soil consolidation due to piezometric level depletion caused by excessive pumping of groundwater. The study area is part of Segura River valley located in the oriental sector of the Betic Cordillera. Permian and Triassic deformed materials corresponding to the Internal Zones of the Betic Cordillera make up the basement. The basin filling comprises Upper Miocene to Quaternary sediment fluvial deposits. Younger sediments are highly compressible and the most problematic from a geotechnical point of view [4]. They constitute an aquifer system that is divided in two units. The superficial aquifer reaches 30 meters below the surface, and it is formed by recent clay, silt and sands facies. The deep aquifer, located below, is composed of a sequence of gravels and sands alternating with confined silt and clay layers. Subsidence is triggered by the excessive water pumping of the first layer of deep aquifer. In fact a piezometric level decline between 5 and 15 m was measured on this layer during recent

drought periods: 1980–1983, 1993–1995 and 2005–2008. After the second drought period, ground subsidence was triggered causing damages in buildings and other structures with an estimated cost of 50 million Euros, generating a significant social impact. As a consequence, a permanent monitoring has been carried out since then, by using an extensometer network since 2001 and also through the application of different PSI [5]. Figure 1 shows the distribution of the compressible thickness and the maximum groundwater depletion in the period 2004-2008 and the wells distributed along the city.

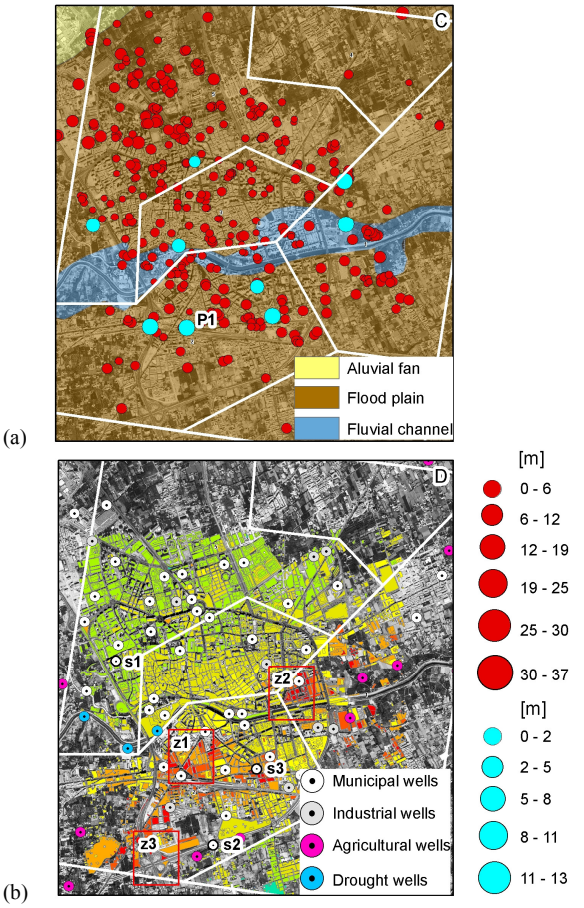

Figure 1 (a) Geology with superposition of the distribution of the compressible thickness (red circles) and the maximum groundwater depletion in the period 2004-2008 (blue circles). (b) Subsidence rate measured from TerraSAR-X dataset interpolated for every building block of the city and location of the different types of wells

4 TerraSAR-X and ERS/ENVISAT datasets comparison

From one side, the results presented in this work have been obtained with 39 TerraSAR-X images acquired during the temporal interval comprised from 28/06/2008 to 25/11/2009. From the dataset of 39 TerraSAR-X images, interferograms have been generated with spatial baselines ranging from 7 m to 295 m. From the other side, 4 ERS and 14 ENVISAT images covering the period from 28/06/2008 to 05/12/2009 have been used for comparison purposes. From them, 4 interferograms ERS and 44 ENVISAT have been formed with baselines ranging from 3 m to 203 m. The reduced number of images for the latter case does not allow to retrieve a very reliable non-linear deformation pattern and thus comparison between the two datasets has been limited to the linear velocity of deformation. In the processing different types of pixel selection methods have been used, such as coherence or amplitude stability. The different methods have allowed the identification of different types of targets, from deterministic to distributed. In some cases, and due to the different resolutions of the images, different behaviours can be observed in the same area depending on the sensor used.

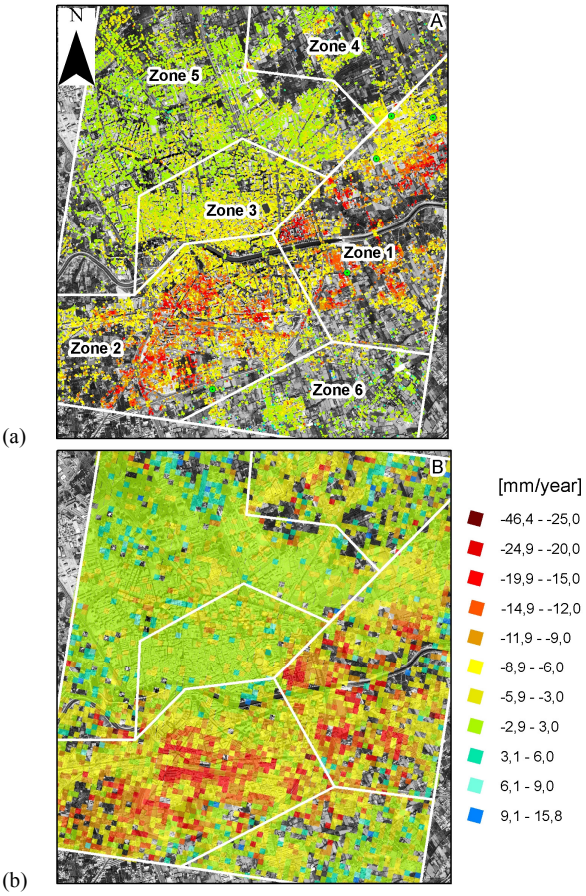

Figure 2 Linear velocity retrieved for Murcia test-site using (a) TerraSAR-X and (b) ERS/ENVISAT data.

In order to compare results retrieved from both datasets the study area has been divided into six zones, see Figure 2 (a). The deformation results are very similar for both sensors, i.e. subsidence areas are found in the same places and with similar rates, as it can be seen in Figure 2. The main differences are highlighted on particular deformations that can be detected with TerraSAR-X, thanks to its better resolution, but cannot be

seen with ERS/ENVISAT data. For instance some buildings that were hardly identifiable in the ERS/ENVISAT results are clearly seen with TerraSAR-X as shown in the example of Figure 3.

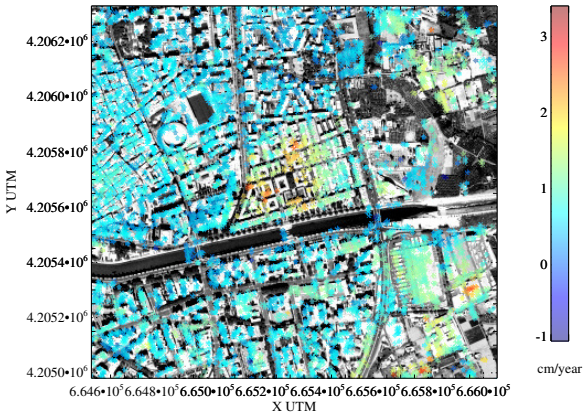

(a)

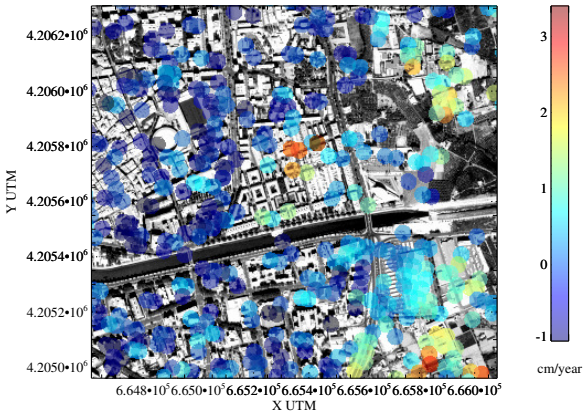

(b)

Figure 3 Deformation in a group of buildings near Segura River. The benefits of the higher resolution of TerraSAR-X can be clearly seen.

Another interesting example of the excellent performance of TerraSAR-X for monitoring civil infrastructures can be seen in Figure 4. The deformation is detected on the access ramps of the bridge, which do not have such strong and deep foundations as the bridge over the highway. The piles of the bridge make this part of the structure less susceptible to experiment settlements, and hence measured deformation on the bridge is below 5 mm/year, which is the lowest value along it. This phenomenon is a common problem due to the construction technique employed.

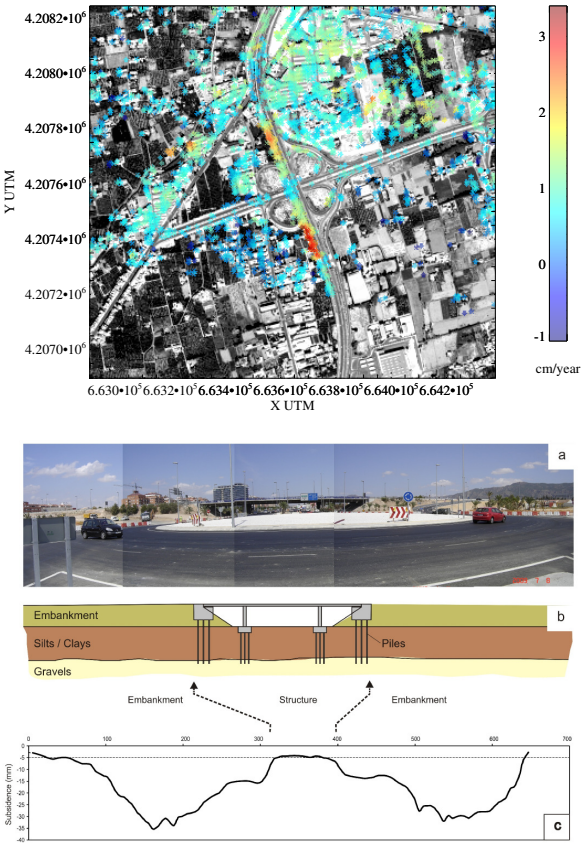

Figure 4 Detail of the bridge over the highway. The deformation on the access ramps is clearly visible while the bridge itself is perfectly stable as seen in the deformation profile along the bridge.

	Zone 1	Zone 2	Zone 3	Zone 4	Zone 5	Zone 6
X-band [CPs/km2]	1999	2662	4180	1461	2762	1217
C-band [CPs/km2]	226	253	269	212	243	206
Def. TSX [mm/year]	-7.3 ± 4.3	-7.1 ± 5.3	-3.6 ± 2.3	-2.8 ± 3.4	-1.9 ± 2.4	-1.6 ± 3.6
Def. Envisat [mm/year]	-5.7 ± 5.7	-6.9 ± 5.3	-1.6 ± 3.1	-2.6 ± 4.7	-0.8 ± 3.8	-2.7 ± 4.8
Difference [mm/year]	1.6 ± 1.4	0.2 ± 0	1.9 ± 0.8	0.2 ± 1.3	1.1 ± 1.4	1.1 ± 1.2
Nº. Geotech. Boreholes	57	79	66	3	177	2
Soft soil thickness [m]	14.9 ± 7.1	14.7 ± 5.4	11.1 ± 4.7	10.2 ± 4.0	14.1 ± 5.6	22.9 ± 1.8
Piez. Var. 04-08 [m]	-9.2	-8.9	-6.6	-8.4	-4.8	
Piez. Var. 08-09 [m]	+3.2	+3.3	+2.9	+2.5	+0.5	

Table 1 Results of the analysis made in each of the six zones defined in Murcia City.

In the first two rows of Table 1 we observe that there is a greater variation of the density of the CPs detected in each of the six zones for the X-band dataset than for the C-band, e.g. in the city centre (zone 3 in Figure 2

(a)) X-band provided 4180 CPs/km2 against 267 CPs/km2 in the case of the C-band, whereas in a sub-urban and agricultural area (zone 6 in Figure 2 (a)) this relation was 1217 against 206 CPs/km2. This difference can be explained considering the nature of the microwave signal: the wavelength of C-band is 5.6 cm while at X-band is 3 cm. The shorter the wavelength the more sensitive is the interferometric phase to the different decorrelation factors induced by changes in the scene. Thus, C-band data is able to provide a better coverage in non-urban areas with bare soil or low vegetation. On the contrary and for this same reason, in urban areas the better resolution of X-band data is able to provide a greater amount of observations. The average and standard deviation of the subsidence rate of all the CPs included within each of these zones (rows 3 and 4 in Tab.2) show that the difference between measured displacements from X- and C-band datasets is 1.0 ± 1.2 mm/year.

5 Conclusions

The Coherent Pixel Technique (CPT) has been successfully used to detect and monitor recent subsidence affecting Murcia city by exploiting and comparing two datasets available from C- and X-band satellite radars. The X-band data yielded a much denser measurement point distribution but a lower spatial coverage, being more adequate for local deformation phenomena analysis than the C-band, especially if we consider the higher cost of the SAR images of the former. The spatial distribution and the magnitude of measured deformation rate have been proven to be very similar by comparing both datasets (1.0 ± 1.2 mm/year) for every proposed zone, as well as for every C-band pixel. It has been observed that 74 % of the C-band CPs measurements coincide with the range of X-band CPs measurements ± 1 mm/year. On the other hand, the comparison of X-band and extensometer measurements indicates their capability for detecting sensible variations of small ground surface deformations.

The spatial analysis of X-band measured subsidence has permitted to demonstrate that settlement areas are located within the flood plain of the valley close to the River Segura where: the soft soil is thicker, the maximum piezometric decline has occurred; and the agricultural and drought pumping wells are located. The comparison of C- and X-band displacement time series with the piezometric temporal evolution has permitted to demonstrate that the 11 days temporal sampling of the X-band dataset permits to detect seasonal variations of ground surface displacement that cannot be detected with the C-band analysis.

Finally one example of ground surface deformation analysis in infrastructures has been presented. This example illustrates that the X-band spatial resolution permits to identify the differential settlement caused when the foundations of buildings and infrastructures off different types are joined, such as the settlement mechanisms governing the different parts of the highway bridge.

6 Acknowledgement

This work has been supported by the Spanish MICINN and European Union FEDER funds under project TEC2008-06764-C02. The TerraSAR-X images were provided by DLR in the framework of the scientific project GEO0389. ERS and ENVISAT data were provided by ESA in the framework of the CAT1 1 project 2494. The Cartographical Service of Murcia (CARTOMUR) has provided the DEM and orto-images used in this work.

References

[1] Ferretti, A., C. Prati, Rocca, F. (2000). Nonlinear subsidence rate estimation using permanent scatterers in differential SAR interferometry. IEEE Transactions on Geoscience and Remote Sensing 38, 2202-2212.

[2] Berardino, P., Fornaro, G., Lanari, R., Sansosti, E. (2002). A new algorithm for surface deformation monitoring based on small baseline differential SAR interferograms, IEEE Transactions on Geoscience and Remote Sensing 40, 2375-2383.

[3] Blanco, P., Mallorquí, J.J., Duque, S., Monells, D. (2008). The Coherent Pixels Technique (CPT): an Advanced DInSAR Technique for Non-linear Deformation Monitoring, Pure and Applied Geophysics 165, 1167-1193

[4] Mulas, J., Aragón, R., Martínez, M., Lambán, J., García-Arostegui, J.L., Fernández-Grillo, A.I., Hornero, J., Rodríguez, J., Rodríguez, J.M. (2003). Geotechnical and hydrological analysis of land subsidence in Murcia (Spain). Proc. 1ª International Conference on Groundwater in Geological Engineering, 22-26 September 2003, Bled, Slovenia, 50, 249-252.

[5] T. Roberto, Y. Márquez, J.M. López Sánchez, J. Delgado, P. Blanco, J.J. Mallorquí, M. Martínez, G. Herrera, J. Mulas (2005), Mapping ground subsidence induced by aquifer overexploitation using advanced Differential SAR Interferometry: Vega Media of the Segura River (SE Spain) case study, Elsevier Remote Sensing of Environment, Vol. 98, pp. 269-283, August 2005.